Line shapes and decay dynamics of dissociative resonances above the second dissociation limit of molecular hydrogen

C. H. Cheng, J. T. Kim, and E. E. Eyler
Physics Department, University of Connecticut, Storrs, Connecticut 06239

N. Melikechi
Department of Physics and Astronomy, Delaware State University, Dover, Delaware 19901

(Received 11 September 1997)

We have systematically studied the line shapes and dynamics of several dissociative resonances near the second dissociation limits of H_2, D_2, and HD. Spectral overlap is eliminated using laser double resonance through the $EF\ ^1\Sigma_g^+$ state, and state-selective detection is used to distinguish dissociation to the $H(1s)+H(2s)$ and $H(1s)+H(2p)$ channels. The threshold region contains both dissociative Rydberg states belonging to the $3p$ complex and shape resonances from the B, B', and C states. Line shapes range from nearly symmetric to highly asymmetric, and most fit well with Beutler-Fano profiles. The observed linewidths of near-threshold shape resonances are in strong disagreement with nonadiabatic theoretical calculations. In some instances, broad resonances coincide almost exactly with the dissociation thresholds, greatly affecting the cross sections and dissociation dynamics. An unusual resonance in HD is observed, in which the $H(2s)$ cross section exhibits a strong interference line shape at the position of the threshold for $D(2s)$ production. [S1050-2947(98)08002-0]

PACS number(s): 33.70.Jg, 33.80.Gj, 33.40.+f

I. INTRODUCTION

The second dissociation limit of molecular hydrogen, converging to $H(1s)+H(2s$ or $2p)$, exhibits surprising complexity, partially because of the near degeneracy of the $n=2$ atomic levels. Some time ago, our research group reported results from a laser double resonance experiment showing numerous resonances both below the dissociation limit and in the continuum immediately above it [1]. The detection scheme used for this work suffered major limitations, reducing the experimental resolution and in some cases distorting the continuum structure. We have now completed an extensive program of experimental studies using improved detection methods that provide sensitive and selective detection of $H(2s)$ and $H(2p)$ atoms with no observable power broadening of the molecular spectra. This paper is the first of a series presenting the results. It describes high-resolution studies of resonances embedded in the near-threshold dissociation continuum. Subsequent papers will deal with the bound-state spectrum and with the determination of accurate new values for the dissociation energies.

The emphasis in this work is on obtaining fully resolved spectra of selected features in the first 50 cm^{-1} above the dissociation threshold, a region in which threshold behavior and long-range interatomic interactions play an important role. Some of the features we report have previously been observed by other methods. Early work by Monfils and by Namioka [2–4] was sufficient to assign the most prominent spectral features, but not to observe line shapes or the photodissociation continuum. The first close look at the threshold region came in 1970, when Herzberg used a 10.5-m vacuum spectrograph to measure total ground-state photoabsorption of H_2, D_2, and HD with a resolution better than 1 cm^{-1} [5]. He determined the dissociation energy from the threshold onset, but could not fully assign the near-threshold resonances because of difficulties with overlapping rotational transitions. At about the same time, Comes and Schumpe studied the line shapes of resonances to the Rydberg $D(3p\pi)\ ^1\Pi_u$ state in H_2 and D_2 [6]. This state undergoes predissociation for $v \geqslant 3$ in H_2 and $v \geqslant 4$ in D_2 due to interaction with the $B'\ ^1\Sigma_u^+$ state. Further major progress occurred in the 1980s, when Glass-Maujean, Breton, and Guyon obtained an extensive map of the entire threshold region of H_2 with a resolution of about 8 cm^{-1} [7]. Their work included separate observations of absorption, molecular fluorescence, and Lyman-α radiation from predissociated $H(n=2)$ atoms. This work, which used dispersed synchrotron radiation, revealed the overall dynamics of a broad range of molecular states but did not have sufficient resolution to investigate the immediate region of the dissociation threshold.

The present generation of experiments began in 1989 when McCormack and Eyler successfully demonstrated laser double-resonance excitation of the threshold region through the $EF\ ^1\Sigma_g^+$ state [8,9]. The relevant potential curves are shown in Fig. 1. Improved results were obtained by Melikechi and Eyler [1], who used a separate detection laser tuned to the hydrogen Balmer-α transition to monitor $H(2s)$ or $H(2s+2p)$ atoms. Balakrishnan and Stoicheff took an alternative approach, using laser-generated vacuum ultraviolet (VUV) radiation to directly measure the second dissociation limit from the ground state [10,11]. All three laser experiments revealed a strong resonance just above the $N''=1$ threshold in H_2, although no serious attempt was made to analyze it, and the double resonance work revealed considerable additional structure. The present paper is a direct successor to our 1993 work, and it includes previously unreported results from the earlier work in addition to our new measurements.

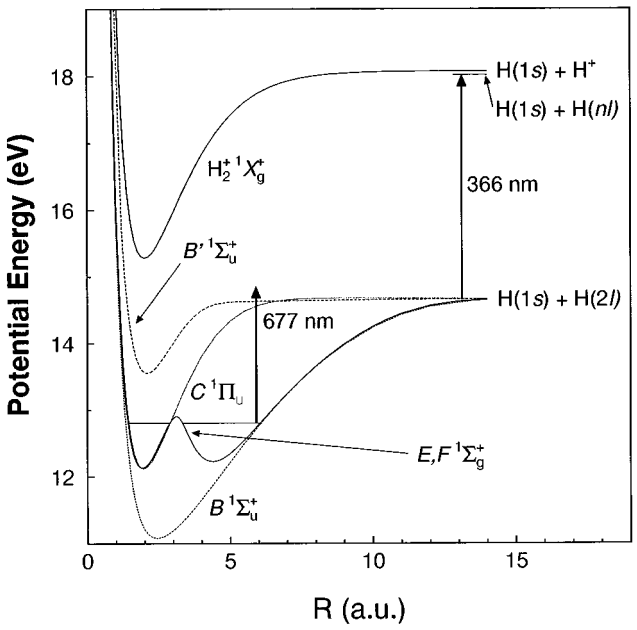

FIG. 1. Potential curves near the second dissociation limit. The B and C states converge adiabatically to H($2p$), while the B' state converges to H($2s$).

There is apparently only one theoretical treatment of the immediate threshold region, a simple adiabatic calculation by Zucker and Eyler [12]. They determined photodissociation cross sections from the EF state and showed that in the adiabatic approximation, the structure in the first 100 cm^{-1} should be completely dominated by the B'state. They also pointed out that the threshold law behavior of the photodissociation cross section is greatly modified if a shape resonance occurs near the threshold, with large deviations from the Wigner threshold law starting less than 1 cm^{-1} above the dissociation energy.

Other photodissociation calculations have concentrated on the behavior of the cross sections over a broad range of energies further above threshold. In 1969 Allison and Dalgarno calculated adiabatic photodissociation cross sections from the ground state into the B, B', and C continua of H_2 [13], and in 1986 Glass-Maujean carried out an improved calculation of the same type [14]. Glass-Maujean and co-workers also calculated $2s{:}2p$ branching ratios both at shape resonances and for the underlying continuum [15], showing that quantum interference can cause slow oscillations in the branching ratio as a function of energy. The results are in fairly good agreement with related experiments [16,17].

For a few of the photodissociation resonances more sophisticated theoretical treatments are also available. Recently Burciaga and Ford conducted a nonadiabatic calculation of resonances in the $C\ ^1\Pi_u$ state in H_2, including the effects of interaction with the $B\ ^1\Sigma_u^+$ state [18]. We report experimental results for two of the resonances they calculated. A number of detailed theoretical studies of photodissociation to the $D(3p\pi)\ ^1\Pi_u$ have been published [15,19,20]. Higher above the threshold edge, a voluminous literature exists, and we make no attempt to summarize it here.

The continuum resonances described in this work include the strongest resonances observed within a few tens of wave

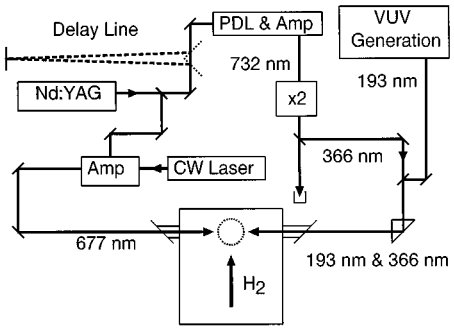

FIG. 2. Experimental configuration for state-selective H atom detection. Apparatus labeled ''VUV generation'' contains a second dedicated Nd:YAG laser. PDL denotes a pulsed dye laser.

numbers above the thresholds of H_2, D_2, and HD, as well as other selected resonances chosen to answer specific physical questions. These resonances can be broadly grouped into three types: threshold resonances, shape resonances, and dissociative Rydberg states. The first of these classifications is an unconventional one, a distinction we make because in some cases we observe strong resonances lying so close to the dissociation limit that they dominate the threshold behavior. Analogous behavior is seen in studies of photoassociation spectra of alkali dimers, where shape resonances have in some cases been observed extremely close to threshold [21,22]. In H_2 the most obvious example is the previously mentioned resonance at the $N''=1$ threshold. It was noted by Herzberg in his 1970 study of ground-state photoabsorption in H_2 [5] and was attributed by him to the C, $v=13$, $N=2$ level. In this paper we show that there are actually two strong resonances at this threshold, the first due to the C state and the second to the B'state. We also describe a somewhat different type of threshold resonance in the HD molecule, as well as line-shape studies for several shape resonances and Rydberg resonances.

II. EXPERIMENT

The experimental setup is sketched in Fig. 2. With the exception of the detection scheme, it is similar to that of Ref. [1]. A pulsed supersonic beam of molecular hydrogen is collimated and then passes into a differentially pumped interaction region, where it is crossed at right angles by two or more lasers. A broadband pump laser at about 191 nm excites selected levels of the EF state with energies near the barrier of the double-minimum potential well. Subsequently a narrow-band probe laser at 677 nm excites the molecules to the region of the second dissociation limit.

The pump and probe lasers are similar to those used for Refs. [1,9]. To produce the 191-nm pump light, the output of a 705-nm pulsed dye laser is mixed in a BBO crystal with fourth-harmonic radiation from a Nd:YAG laser. The 677-nm probe light is produced by pulsed amplification of a cw dye laser. The 191-nm and 677-nm beams are derived from dye lasers using separate Nd:YAG pump lasers, so the relative delay is electronically adjustable. A delay of 60 ns was typically employed. The probe pulse, 6 ns in duration, is focused to a typical diameter of 0.7 mm, and we varied its energy from 15 μJ to 2 mJ depending on the strength of

individual transitions. The obtainable resolution is determined by the bandwidth of the 677-nm laser, approximately 90 MHz, and by the residual transverse Doppler width, approximately 25 MHz for our highest-resolution work. For all of the spectral features reported in this paper, the experimental resolution is much narrower than the observed linewidths and can be neglected entirely.

Two detection schemes were used in this work. The C state shape resonances reported in Secs. IV B, V A, and V B were observed using direct multiphoton ionization, detecting H^+ ions produced by the 677-nm probe laser. The remainder of the results were obtained using state-selective detection of $2s$ or $2p$ atoms with a third laser. The state-selective detection is accomplished in a stepwise fashion. First a laser at 366 nm is used to excite the $n=2$ atoms to $n=40$ high Rydberg states, then the Rydberg atoms are detected by delayed pulsed field ionization. The $2s$ hydrogen atom is metastable with a lifetime about 1/7 s. On the other hand, the $2p$ lifetime is only 1.6 ns. Thus we can operate the probe and detection lasers in coincidence to detect both $2s$ and $2p$ atoms, or we can delay the detection laser to detect $2s$ atoms alone. This Rydberg detection scheme significantly reduces the power requirements for the probe and detection lasers compared with direct multiphoton ionization (MPI) detection [1,9]. Therefore power broadening is nearly eliminated and sensitivity is improved.

The detection laser is a modified Molectron DL II pulsed dye laser operating at 732 nm with a bandwidth of about 0.5 cm^{-1}. Its output is further amplified in a transverse dye cell, then frequency doubled in potassium dihydrogen phosphate (KDP) to produce about 1 mJ in a 6 ns pulse at 366 nm. This detection laser is pumped by the same Nd:YAG laser as the 677-nm probe beam. To provide a suitable delay for $2s$ atom detection, a 40-ns delay line was inserted in the Nd:YAG beam path. The mirror position was indexed so that switching between coincident and delayed detection could be accomplished in less than 3 min. The major advantage of delaying the Nd:YAG pump laser instead of dye laser itself is to minimize the change of detection laser beam alignment. The pulsed electric field for Rydberg atom detection is provided by a homemade pulser producing 500-ns, 400-V/cm pulses, fired 1 μs after the detection laser. A weak dc electric field of ≈ 10 V/cm is also present, to eliminate stray ions produced by the pump laser alone.

Ions were detected by a fast discrete-dynode electron multiplier, with a short time-of-flight region to allow mass discrimination. To reduce the effects of slow intensity fluctuations we typically average the results of three independent scans. All of the figures in this paper show the averaged results unless otherwise indicated.

III. DATA ANALYSIS AND LINE-SHAPE RESTORATION

A. Extracting the $2s$:$2p$ branching ratio

As described in Sec. II, our detection scheme measures only $2s$ atoms if the detection laser is delayed by 40 ns, while both $2s$ and $2p$ atoms are detected if there is no delay. We expect predominantly $2s$ atoms in the near-threshold continuum, since in the adiabatic approximation the cross sections are dominated by the B' state, which converges to $H(1s)+H(2s)$. This is generally what we observe, and is consistent with a lower-resolution study of ground-state photodissociation by Mentall and Guyon [16]. However, exceptions can occur when nonadiabatic effects are important, or where resonances to the B and C states occur. We have explicitly studied the $2s$:$2p$ branching ratio for the near-threshold continuum of H_2 with $N''=1$, where resonances to both the C and B' states occur within the first 5 cm^{-1}. Unfortunately we have not yet obtained sufficient data to carry out a complete analysis for any of the other resonances reported here.

To quantitatively compare the $2s$ and $2p$ cross sections, a three-step procedure is used: (1) Determine the relative detection efficiency for $2s$ atoms when using the coincident $(2s)$ and delayed $(2s+2p)$ detection schemes. (2) Subtract the appropriately scaled $2s$ spectrum from the $2s+2p$ spectrum to obtain the $2p$ spectrum. (3) To determine the $2s$:$2p$ branching ratio, we must also allow for the possibility that within the $2s+2p$ spectrum, the detection efficiencies for $2s$ and $2p$ may differ.

The remainder of this section describes the details of this procedure:

Step 1: The detection efficiency for $2s$ atoms should be nearly the same for prompt and delayed detection, but there can be small changes because of collisional loss of $2s$ atoms, because the interaction time with an average $2s$ atom is shortened when the probe and detection pulses coincide, and finally because the detection laser is sufficiently powerful to slightly deplete the EF state via direct photoionization. The first problem is eliminated by using a fairly short (40 ns) delay time, and the second is minimized by using sufficient power to saturate the $2s$ to $40p$ transition under all experimental conditions. We also made an experimental determination of the relative detection efficiency by observing the D_2, $N''=0$ continuum just above threshold using both prompt and delayed detection. We are confident that this continuum dissociates only to $D(2s)$ atoms for two reasons: the cross sections for $2s$ and $2s+2p$ detection are identical in shape, and the bound-state spectrum shows no sign of effects due to nonadiabatic coupling of the B' state with the B or C states.

Step 2: Comparing the $D(2s)$ signals for coincident and delayed detection, we find that the efficiency of coincident detection is slightly lower, about 87% of the delayed detection efficiency, with a statistical uncertainty less than 0.01. This gives us the information we need to subtractively obtain the $2p$ spectrum.

Step 3: Although we ascertained that the atomic $2s$-$40p$ transition is saturated (experimentally we observed that the laser was at three times the saturation irradiance), the $2p$ atoms are harder to detect. The matrix elements for the $2s$-$40p$ and $2p$-$40d$ transitions are nearly the same, but the $2p$ atoms decay in just 1.6 ns, limiting the interaction time with the 6-ns laser pulse. Combining this information, we estimate that the $H(2p)$ atoms are detected with an efficiency ≈ 0.7 times the $2s$ detection efficiency.

B. Dissociation and Beutler-Fano line shape

If a single bound level interacts with a single flat continuum, the resonance line shape can be described by the familiar Beutler-Fano profile [23],

$$\sigma(\omega)=\frac{A[q+(\omega-\omega_0)/(\Gamma/2)]^2}{1+[(\omega-\omega_0)/(\Gamma/2)]^2}, \tag{3.1}$$

where ω_0 is the resonance frequency, Γ the parametrized linewidth, q the asymmetry parameter, and A the amplitude. The asymmetry parameter q is proportional to the ratio of the dipole matrix elements coupling the initial state to the dissociative bound level and to the continuum. It is worth noting that the peak frequency ω_p and the peak strength $\sigma(\omega_p)$ are given not by ω_0 and A but by

$$\omega_p=\omega_0+\frac{\Gamma}{2q}, \tag{3.2}$$

$$\sigma(\omega_p)=A(q^2+1). \tag{3.3}$$

The assumptions underlying Eq. (3.1) are not satisfied for all of the resonances described in this paper, because in some cases the underlying continuum is not flat, or more than one dissociation continuum is present. Nevertheless, we have found that the Beutler-Fano line shape provides an excellent empirical fit to all but a few of the resonances we report, though in some cases an offset is needed to allow for the presence of noninteracting continua.

C. Depletion broadening

In some cases the spectra are distorted perceptibly by depletion broadening. This effect occurs if a substantial fraction of the available EF state molecules are excited at the line center, reducing the peak signal size. We have improved the method of Nussenzweig *et al.* [24] to correct this lineshape distortion for noisy data. The strategy here is to measure the level of depletion first. The quantified depletion effect is then incorporated into a least-square fitting routine to determine the corrected line shape.

Taking into account the fact that our laser bandwidth is much narrower than the transition width, we define the depletion parameter as

$$f(\omega)=1-\exp\{-I_0\sigma(\omega)\}, \tag{3.4}$$

where I_0 is proportional to the laser irradiance and $\sigma(\omega)$ is the excitation cross section. It is clear that $f(\omega)$ is the fraction of molecules being depleted from the lower state by the laser pulse. Moreover the observed signal strength $G(\omega)$ is linearly proportional to the number of excited molecules, so that if ω_p is the laser frequency at the signal peak,

$$\frac{G(\omega)}{G(\omega_p)}=\frac{f(\omega)}{f(\omega_p)}. \tag{3.5}$$

We can rewrite Eq. (3.4) to express the scaled laser irradiance I_0 in terms of $f(\omega)$ and $\sigma(\omega)$ at the signal peak ω_p:

$$I_0=-\frac{\ln[1-f(\omega_p)]}{\sigma(\omega_p)}. \tag{3.6}$$

It is straightforward to substitute Eqs. (3.4) and (3.6) into (3.5) to obtain

$$G(\omega)=G(\omega_p)\frac{1}{f(\omega_p)}\left\{1-\exp\left[\ln[1-f(\omega_p)]\frac{\sigma(\omega)}{\sigma(\omega_p)}\right]\right\}. \tag{3.7}$$

For a given line shape $\sigma(\omega)$ the ratio $\sigma(\omega)/\sigma(\omega_p)$ is known. Therefore it is sufficient to only measure $f(\omega_p)$ to define the relation between the true line shape $\sigma(\omega)$ and the broadened line shape $G(\omega)$ within a multiplicative constant $G(\omega_p)$.

However, it is not practical to correct noisy data on a point-by-point basis using Eq. (3.7), because the noise is greatly amplified by the desaturation process. Instead we use a nonlinear least-squares fitting routine to find the best fit of the depleted line shape $G(\omega)$ to the data. The fitting program varies both the peak amplitude $G(\omega_p)$ and the parameters describing the line shape $\sigma(\omega)$ (in our case, a Beutler-Fano profile). The resulting parameters of $\sigma(\omega)$ are fully corrected for depletion broadening. The fit results $G(\omega)$ are also easily compared with the raw data by eye to ascertain that they indeed provide a good smoothed representation of the data. If desired, one can then rescale the amplitude of each data point by the ratio of $\sigma(\omega)/G(\omega)$ to calculate a depletion-corrected data file. This method of treating depletion broadening is easy to implement and robust against noise, and is applicable whenever the parametric form of the line shape $\sigma(\omega)$ is known.

D. Uncertainty of the asymmetry parameter

The confidence interval for q is not centered around the best-fit value, a problem that becomes severe when the line shape is nearly symmetric. This problem occurs because the line shape changes little for values of q higher than about 20, so a large positive change in q is needed to effect the same change in χ^2 as a small negative change. (A similar argument applies to large negative values of q.) In the work reported in this paper, this poses problems in just one case, the C, $v=13$, $N=3$ shape resonance in H_2. To estimate the uncertainty in this case we first chose a conservative lower bound for q based on examination of the scatter between fits to repeated line scans. We then conducted least-squares fits with q fixed at a wide range of different values, allowing all other fitting parameters to vary. The upper bound for q is determined by requiring that it gives the same result for χ^2 as the lower bound.

IV. THRESHOLD RESONANCES

A. The $N''=1$ threshold of H_2: $C^1\Pi_u^+$ $v=13$, $N=2$ and B' $^1\Sigma_u^+v=9$, $N=2$

The $N''=1$ threshold for the H_2 isotopic variant is especially interesting because we observe two strong resonances that nearly coincide with the dissociation energy, modifying the threshold behavior and causing large nonadiabatic effects. Past assignments of energy levels in this region have been ambiguous. The $C\ ^1\Pi_u$ $v=13$, $N=2$ level was first assigned by Namioka [3] with a term energy of 118 379 cm^{-1}, and subsequent work has retained this assignment. The B', $v=9$ state has suffered a far more confused history. Namioka initially placed the $N=1$ level at 118 365.45 cm^{-1} and the $N=2$ at 118 365.99 cm^{-1}. Dabrowski and Herzberg reassigned the $N=1$ level much higher, at 118 376.12 cm^{-1}

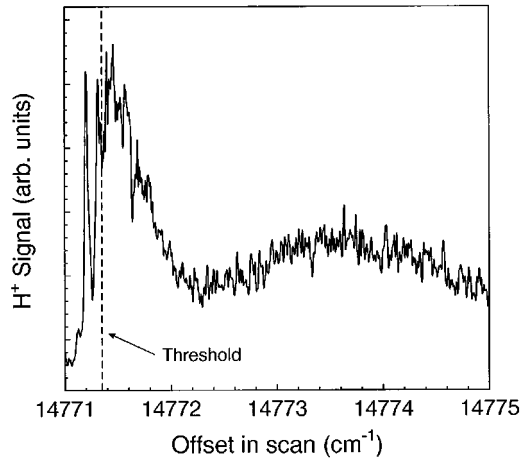

FIG. 3. Survey scan of the $N''=1$ threshold region of H_2. This signal was obtained by MPI production of H^+ ions, and is slightly power broadened by the probe laser. Resonances to C, $v=13$, $N=2$ and B', $v=9$, $N=2$ are clearly observed.

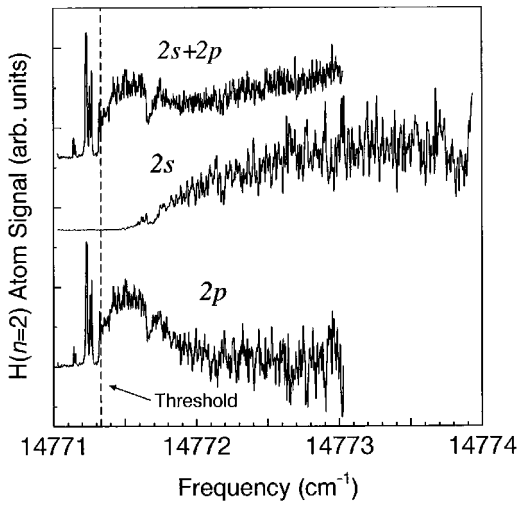

FIG. 4. Comparison of $2s$ and $2p$ atom production near the $N''=1$ threshold of H_2. Upper plot shows $2s+2p$, observed with coincident probe and detection laser pulses, while the middle plot shows $2s$ only, observed with a delayed detection pulse. The bottom plot showing $H(2p)$ production was obtained as described in the text. These plots are from a single experimental scan, not a three-run average.

[25]. However, Stwalley later assigned this same spectral feature to the B , $v=39$, $N=1$ level [26], and later still, Senn *et al.* reassigned it back to B', $v=9$, $N=1$ [27]. The B', $v=9$, $N=2$ level has gone unassigned ever since Namioka's analysis proved incorrect, although Zucker and Eyler pointed out that it should correspond to a strong shape resonance just above threshold [12]. Such a resonance was first reported experimentally in the VUV laser experiment of Balakrishnan *et al.* [10], who monitored $H(2s)$ production via Lyman-α fluorescence.

We have resolved this confusion by determining that there are in fact two previously unresolved resonances just above threshold, one decaying to $H(2s)$ associated with B', $v=9$, $N=2$ state and the other to $H(2p)$ associated with C , $v=13$, $N=2$. Figure 3 shows the whole threshold region at low resolution using MPI detection, and clearly indicates the double structure. The sharp peaks below threshold are bound resonances, and will be discussed elsewhere. Comparison with earlier work shows that we have resolved into two components what appeared to be a single peak in Herzberg's 1970 spectrum [5], and that the second peak is the same as the resonance observed in $H(2s)$ production by Balakrishnan *et al.* [10].

Figure 4 depicts high-resolution scans over a slightly smaller region, obtained with our new H atom detection scheme. It shows the $H(2s+2p)$ and $H(2s)$ signals, as well as the derived $H(2p)$ signal, determined as discussed in Sec. III A. In addition to the various corrections described in Sec. III A, we corrected the data for probe laser power variations with an uncertainty of less than 2%. We are confident that the $2s$ subtraction is accurate to within a few percent, so that the bottom trace in Fig. 4 accurately depicts the $H(2p)$ signal. However, the relative size of the $2s$ and $2p$ signals is uncertain by about 25%, introducing a corresponding uncertainty into the $2s{:}2p$ branching ratio. The relative line strength ratio between the two resonances is correspondingly uncertain, with the first $(2p)$ resonance estimated to be larger than the second $(2s)$ by a factor between 0.9 and 1.5.

It is clear from the figures that the first resonance, at 14 771.5 cm^{-1}, dissociates entirely to $H(2p)$ while the second, at 14 773.6 cm^{-1}, dissociates to $H(2s)$. On this basis we can confidently assign the first resonance to H_2, $C\ ^1\Pi_u^+$ $v=13$, $N=2$, which correlates adiabatically to $H(1s)+H(2p)$, and the second to $B'\ ^1\Sigma_u^+$ $v=9$, $N=2$, correlating to $H(1s)+H(2s)$.

Accurate fits to the line shapes are impossible because they lie so close to threshold. In particular, the $H(2p)$ signal has an abrupt onset, and its profile is punctuated by several much narrower resonances. We defer discussion of this threshold structure, which is associated with the atomic fine and hyperfine splittings, to future work.

Even though accurate fits cannot be performed, we can make approximate comparisons of the linewidths with theory. For the B'state, Zucker and Eyler calculate a width of roughly 1.5 cm^{-1}, nearly the same as the observed width. For the C state, Table I shows a comparison with an adiabatic calculation by Burciaga and Ford. While the B'resonance is in good qualitative agreement with theory, the C state resonance is much broader than predicted. We will show in the following sections that this disagreement for the C state linewidth extends to other rotational levels as well.

B. $C\ ^1\Pi_u^-$ $v=13$, $N=2$ in H_2

By exciting the threshold of H_2 from the $N''=2$ level of the EF state, we observe both the continuum onset and a complex threshold resonance as shown in Fig. 5. Unfortunately we have been able to obtain only low-resolution data using MPI detection, a method that yields better signals for very weak transitions. The signal appears to extend slightly below threshold because of power broadening, a typical problem when using MPI detection. Surprisingly, the resonance is observed only in the H_2^+ MPI signal, and not in H^+. We cannot readily account for this observation, which was not typical of other near-threshold levels, but we specu-

TABLE I. Line-shape parameters of selected $C\ ^1\Pi_u^+$, $v=13$ Rydberg states of H_2, ω_0, and Γ in cm^{-1}, q dimensionless.

	This work	Adiabatic, Ref. [18]	Nonadiabatic, Ref. [18]	WKB
$N=2$: ω_0	118380.7	118380.7		
Γ	≈ 0.4	$<2.2\times10^{-5}$		
$N=3$: ω_0	118414.23 (12)	118416.1	118416.4	
Γ	3.56 (29)	0.057	0.097	0.086
q	34 (see text)			

late that the resonance is associated with a comparatively short-range interaction, making ionization probable while the internuclear separation is still small.

We assign this resonance to $C\ ^1\Pi_u^-$ $v=13$, $N=2$. The term energy of the peak is 118 377.6 cm^{-1}. It is in good agreement with the analysis of Senn *et al.* [27], who list the term energy as 118 377.0 cm^{-1}, and only a little higher than the value of 118 376.71 cm^{-1} given by Dabrowski and Herzberg [25]. The line shape is obviously highly asymmetric, and it is even possible that we are observing two overlapping resonances, as we encountered at the $N''=1$ threshold. It is difficult to say more in the absence of further data or detailed calculations.

The line width is roughly 0.15–0.5 cm^{-1}, depending on how one interprets the complex line shape. This is certainly not in agreement with the calculation of Burciaga and Ford, who predict negligible widths for the Π^-components of the C state (a simple WKB tunneling rate calculation gives the same result). We conclude that this level is predissociated by interactions omitted from the Burciaga and Ford calculation. To dissociate this Π^- level requires another state with levels of $(-)$ symmetry, possibly the D state or some other low Rydberg state.

C. Threshold resonance in HD

In the heteronuclear HD isotopomer, the H*+D and H+D* thresholds are separated by 22.4 cm^{-1}. In this experiment, we can easily differentiate H* and D* production by their differing times of flight to the detector. Our observations of the lower threshold are unremarkable, but we observe an unexpected resonance at the upper H+D* threshold, shown in Fig. 6. The line-shape restoration algorithm has been applied to these data to eliminate the effect of depletion broadening as discussed in Sec. III C. The signal size as a function of laser pulse energy was measured independently to determine a saturation factor of $f(\omega_p)=0.970\pm0.009$.

This resonance is highly unusual in that the D* signal at threshold exhibits no resonant behavior (although the sharp continuum onset is not typical of HD). A very strong resonance is observed instead in the H* channel at the D* threshold energy. This feature has apparently never before been observed, although in hindsight a hint of it can be seen in measurements of total photoabsorption by Herzberg [5]. We are unable to associate it with any expected transitions to the B, B', C, or D states, even using the recent theoretical calculations of Senn *et al.* [27]. We are thus forced to tentatively attribute the resonance to nonadiabatic couplings associated with the threshold onset.

The line shape is described well by a Beutler-Fano profile. The effects of our depletion correction process are slight but noticeable, particularly for the asymmetry parameter. Table II gives the results for fits both without corrections and with the depletion corrections.

There is also a hint of a weak, much narrower interference structure between 15 466.16 cm^{-1} and 15 466.34 cm^{-1}, seen in Fig. 6 only as a small deviation from the global Beutler-Fano line profile. The rising edge at 15 466.34 cm^{-1} coincides with the H+D* threshold very closely.

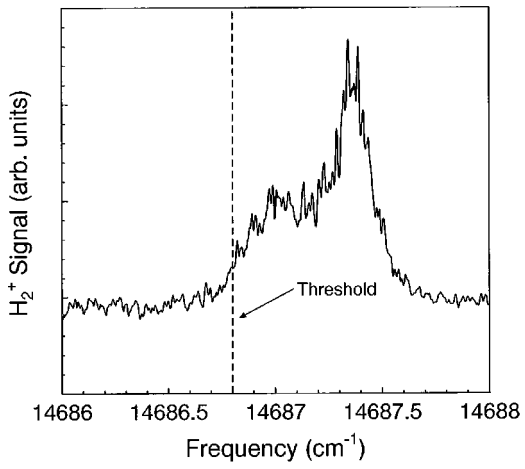

FIG. 5. $N''=2$ threshold region of H_2 detected via MPI to H_2^+, showing C, $v=13$, $N=2$ resonance. The vertical dashed line indicates the dissociation energy. Data are the average of six scans.

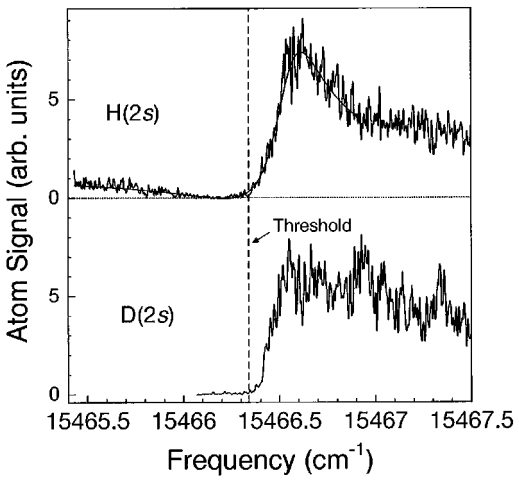

FIG. 6. $N''=0$ threshold of HD, showing H(2s) and D(2s) production in the H+D* threshold region. The smooth solid line superposed on the H(2s) data is a least-squares fit with a Beutler-Fano profile.

TABLE II. Line-shape parameters of the $N''=1$ threshold resonance in HD, dimension the same as Table I.

	Raw data	Depletion compensated
ω_0	118687.26 (8)	118687.32 (8)
Γ	0.392 (30)	0.334 (30)
q	1.0	1.8 (3)

In contrast, no similar phenomena are observed for the $N''=1$ H+D* threshold region, shown in Fig. 7. For these data no observable saturation is found, so no correction is needed. The H* continuum is flat throughout the region of the H+D* threshold apart from a monotonic decline, which may be partially due to competition from D* atom production [15]. The shape of the D* threshold is also completely different for $N=1$, exhibiting the gradual rise typical of HD, whose potentials are quite different from H_2 and D_2 at long range because the resonant $1/R^3$ dipole interaction of the B state cannot exist close to the dissociation limit.

V. SHAPE RESONANCES

A. H_2, $C\ ^1\Pi_u^+$ $v=13$, $N=3$

This shape resonance, located 37.7 cm^{-1} above the dissociation limit, is among those included in the nonadiabatic calculation of Burciaga and Ford [18]. We obtained spectra using MPI detection to H^+ ions. Scans were obtained for a 3:1 range of probe laser energies, and analyzed with an early version of our line-shape restoration algorithm (Sec. III A). The saturation parameter f varied from 0.56 to 0.91 for these runs. The observed line shape is very nearly symmetric, as shown in Fig. 8.

Though the scatter is considerable, the fit results show no statistically significant trends with laser power. The averaged values of the line-shape parameters are listed in Table I. As discussed previously the confidence interval for q is highly asymmetric, ranging from about 17 to 2000 with a best-fit value of $q=34$.

Like the other C state resonances in H_2 closer to threshold, the observed linewidth differs greatly from theoretical predictions. Burciaga *et al.* [18] predicted a slightly asymmetric resonance with a width of 0.097 cm^{-1}. Since we excite the resonance from the EF state rather than the ground state directly, the observed q parameter cannot be compared directly to theory, since it depends on a ratio of dipole matrix elements. However, we have generally observed that relative line intensities are very similar to those observed in ground-state photoabsorption, so we would not expect any large change in the line shape of the C state shape resonance. A more reliable comparison is possible for the linewidth, which is almost insensitive to the excitation pathway, especially when q is large. Remarkably, the observed linewidth is 37 times larger than the predicted width, a disagreement that cannot possibly be explained by dependence on the excitation path or by experimental error.

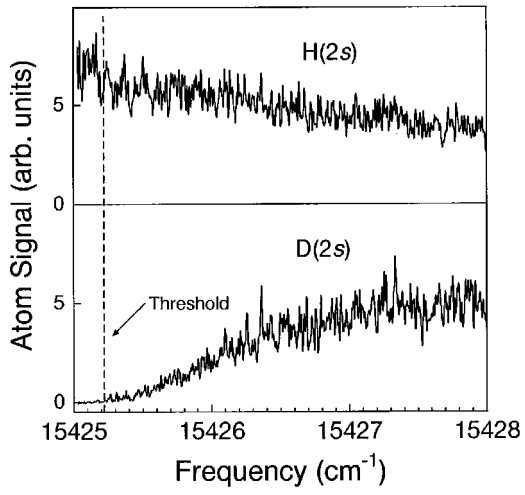

FIG. 7. $N''=1$ threshold of HD, showing H($2s$) and D($2s$) production in the H+D* threshold region.

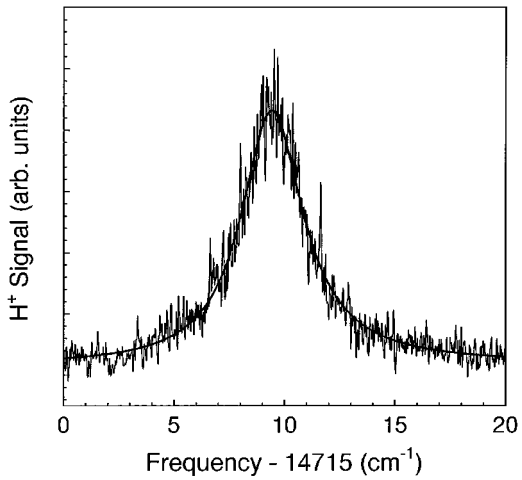

FIG. 8. H_2, C, $v=13$, $N=3$ shape resonance detected in MPI to H^+. The solid line is a least-squares fit with a Beutler-Fano profile.

To further assess this discrepancy, we made an additional rough estimate of the expected linewidth using a simple WKB calculation of the tunneling rate through the C state potential barrier, which peaks at about 9 a.u., where it is about 100 cm^{-1} high. We used the potential curve calculated in 1988 by Wolniewicz [28], which should be slightly more accurate than the older curve used by Burciaga and Ford [29]. As indicated in Table I our result is similar to the Burciaga and Ford calculation. The tunneling rate does not change significantly if the older potential curve is used instead. A third potential curve is available from a calculation by Komasa and Thakkar [30], but again it does not differ sufficiently from earlier work to significantly alter the linewidth of the $N=3$ shape resonance.

There are two possible explanations for the disagreement: either the C state potential curve differs greatly from the calculated potentials, or the effects of nonadiabatic couplings have been grossly underestimated. Because all recent calculations of the potential curve have coincided within 1 cm^{-1}, the latter explanation seems far more likely. Thus we believe that a much more careful theoretical treatment of nonadiabatic interactions at large internuclear separations will be necessary to obtain a good understanding of the near-threshold physics.

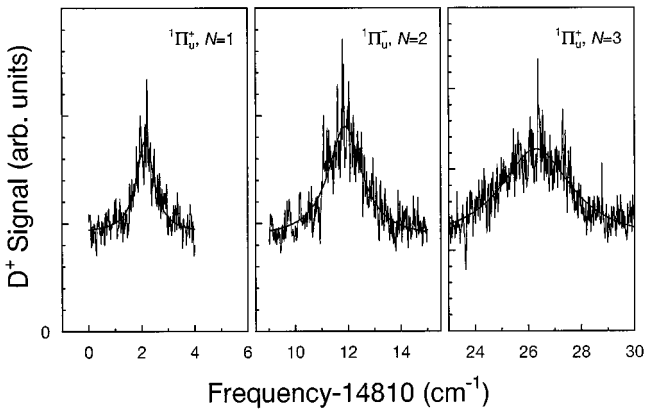

FIG. 9. D_2, C , $v=19$, $N=1,2,3$ shape resonances detected in MPI to D^+. Solid lines are least-squares fits by Lorentzians.

B. D_2, $C\ ^1\Pi_u$ $v=19$, $N=1,2,3$

In deuterium, the $v=19$ levels of the C state lie slightly above threshold, and form resonances analogous to their $v=13$ counterparts in H_2. We were able to observe three rotational levels with $v=19$ by exciting the $P(2)$, $Q(2)$, and $R(2)$ transitions from the $v''=9$, $N''=2$ level of the EF state. These weak transitions were observed only via MPI to D^+ ions. We fitted the spectra to Lorentzian profiles as shown in Fig. 9. The linewidths are listed in Table III, and have large uncertainties due to the limited and noisy data set.

Because nonadiabatic calculations have not been carried out for D_2, we can compare the results only with our WKB estimate of the tunneling rate through the C state barrier. The calculated lifetimes, shown in Table III, are in quite good agreement with the observed widths, considering that the WKB rates can easily be incorrect by a factor of two or more. Moreover, there is no evidence that levels of $(+)$ and $(-)$ symmetry dissociate at different rates. Thus we see no hint in D_2 of the strong and poorly understood nonadiabatic interactions that play such an important role for the corresponding states of H_2.

VI. A PREDISSOCIATIVE RYDBERG STATE: $D(3P)$ $^1\Pi_u^+$ $v=4$, $N=1$ IN D_2

We chose to study the $D\ ^1\Pi_u^+$, $v=4$, $N=1$ level of D_2 because preliminary survey scans showed that it appeared to be anomalously intense and broad. It came to our attention because when scanning the dissociation limit 210 cm^{-1} below, we observed a large background that arose from inadvertent excitation of the D state resonance by broadband amplified spontaneous emission from our laser. Double resonance through the EF , $N''=0$ level provides a D state spectrum free of overlapping lines, shown using $D(2s)$ spectrum in Fig. 10.

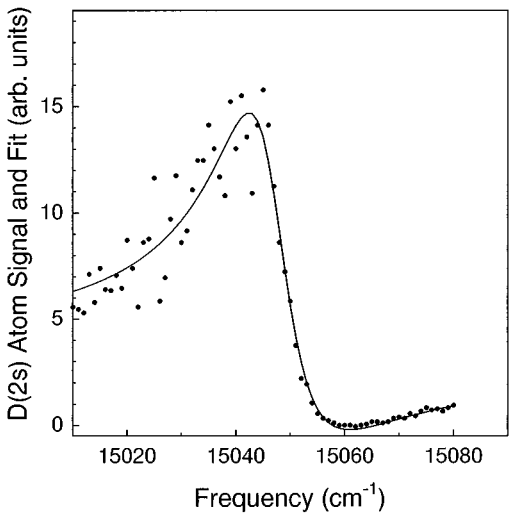

FIG. 10. D_2, $D(3p)$ $^1\Pi_u^+$, $v=4$, $N=1$ Rydberg state detected in $D(2s)$ dissociation channel. Solid line is a least-squares fit with a Beutler-Fano profile.

The D state energy level structure has been well known for many years [2]. The predissociation dynamics were extensively investigated by Comes *et al.* [6]. However, these pioneering studies suffered from a lack of state selectivity as well as poor spectral resolution. In particular, the $R(0)$ and $R(1)$ branches of the (4-0) $D\leftarrow X$ transition in D_2 were not resolved by Comes *et al.* [6], who relied on deconvolution procedures to analyze them. Better measurements were obtained by Glass-Maujean *et al.* [7], but only for H_2. The theoretical work of Beswick *et al.* [15] includes a nonadiabatic calculation of $v=4$ line profiles in both H_2 and D_2. Their calculations for $v=4$ levels in D_2 show that both the linewidth and the asymmetry should increase smoothly with rotation, with predicted widths ranging from 1.1 cm^{-1} for $N=1$ to 11 cm^{-1} for $N=4$.

To our surprise, the resonance is much broader and more asymmetric than expected from the previous measurement or from theoretical predictions (see Table IV). We have verified that our results are independent of the laser power by varying the probe laser power over a 2:1 range, obtaining the same results well within the statistical uncertainty. We do not expect any effect from the small dc electric field used for the experiment, since the term energies are still too low to allow interaction with Rydberg states with $n>4$, and Stark shifts are negligible for these low-n states at 10 V/cm.

The data were analyzed using the procedure of Sec. III. The results are shown in Fig. 10 and Table IV. Clearly the

TABLE III. Line centers and widths of $C\ ^1\Pi_u$, $v=19$, $N=1,2,3$ shape resonances in D_2, in cm^{-1}.

Level	Line center, this work	Line center, Ref. [25]	Width, this work	Width, WKB
$^1\Pi_u^+$, $N=1$	119 085.89(8)	119 085.75	0.8(4)	1.0
$^1\Pi_u^-$, $N=2$	119 095.62(9)	119 095.70	1.6(8)	1.9
$^1\Pi_u^+$, $N=3$	119 110.30(23)	119 110.37	3.3(16)	9.4

TABLE IV. Line-shape parameters of the $D\ ^1\Pi_u^+$, $v=4$, $N=1$ Rydberg state of D_2, dimension the same as Table I.

	This work	Photoabsorption, Ref. [6]	Calculated, Ref. [15]
ω_0	119 243.06 (46)		
Γ	15.0 (9)	<2.3	1.1
q	-1.94 (14)		39

line shape is an excellent fit to a Beutler-Fano profile. However, the disagreement for Γ and q with earlier work is pronounced. The possibility of misidentification seems remote, since our best-fit peak frequency for this resonance, $\omega_p = 119{,}239.20 \pm 0.46\ \mathrm{cm}^{-1}$, agrees very closely with the value of $119{,}239.1 \pm 0.8\ \mathrm{cm}^{-1}$ tabulated by Monfils [2].

Even allowing for the fact that the q parameter may be different for $D \leftarrow EF$ excitation than for $D \leftarrow X$ excitation, we are surprised by both the very strong asymmetry and the broad width. We speculate that this level may interact with a hypothesized shape resonance of the B' or C state, which could account for its anomalous behavior.

VII. CONCLUSIONS

We have observed photodissociation resonances of all three stable hydrogen isotopomers in the near-threshold region by using laser double resonance. High spectral resolution and state selectivity, in both the excitation and detection steps, enable us to study these above-threshold resonances in unprecedented detail. The observed line shapes range from nearly symmetric to highly asymmetric, and most fit well to Beutler-Fano profiles. In a few cases we have obtained high-resolution measurements of the relative cross sections for producing $H(2s)$ and $H(2p)$. This has allowed us to unambiguously assign the $C\ ^1\Pi_u^+ v=13$, $N=2$ and $B'\ ^1\Sigma_u^+$ $v=9$, $N=2$ levels of H_2.

There are several instances where strong resonances occur very close to a dissociation threshold, and in fact this seems to happen in nearly half of the cases we have examined. This close interplay between resonances and dissociation limits appears to reflect the complex dissociation dynamics caused by long-range interactions at the threshold. In most cases where comparison is possible, the observed linewidths strongly disagree with existing nonadiabatic calculation.

The threshold resonance for HD at the upper H+D* limit is of a type apparently not seen previously, in which the H* atom signal exhibits a very strong interference profile coincident with the threshold for D* production. We hope this work will motivate a new theoretical treatment of this system that fully incorporates the coupling between the two dissociation pathways.

Our results for shape resonances higher above threshold also contain some surprises. We observe a much broader line profile for the D, $v=4$, $N=1$ level in D_2 than previous work, apparently because of large errors in the deconvolution procedure used for the earlier measurement. Even more surprising is the behavior of C state resonances in H_2, where the disagreement with recent nonadiabatic calculations seems to persist well above threshold. Clearly a better theoretical treatment of long-range nonadiabatic interactions is needed.

ACKNOWLEDGMENTS

We wish to thank Benjamin Catching for his key role in the experiments on C state shape resonances. This research was supported by the National Science Foundation, Grant Nos. PHY-9318662 and PHY9696038, and by the University of Connecticut.

[1] E. E. Eyler and N. Melikechi, Phys. Rev. A **48**, R18 (1993).
[2] A. Monfils, J. Mol. Spectrosc. **15**, 265 (1965).
[3] T. Namioka, J. Chem. Phys. **40**, 3154 (1964).
[4] T. Namioka, J. Chem. Phys. **41**, 2141 (1964).
[5] G. Herzberg, J. Mol. Spectrosc. **33**, 147 (1970).
[6] F. J. Comes and G. Schumpe, Z. Naturforsch. **26a**, 538 (1971).
[7] M. Glass-Maujean, J. Breton, and P. M. Guyon, Z. Phys. D **5**, 189 (1987).
[8] E. F. McCormack, Ph.D. thesis, Yale University, 1989.
[9] E. F. McCormack and E. E. Eyler, Phys. Rev. Lett. **66**, 1042 (1991).
[10] A. Balakrishnan, V. Smith, and B. Stoicheff, Phys. Rev. Lett. **68**, 2149 (1992).
[11] A. Balakrishnan, V. Smith, and B. P. Stoicheff, Phys. Rev. A **49**, 2460 (1994).
[12] C. W. Zucker and E. E. Eyler, J. Chem. Phys. **85**, 7180 (1986).
[13] A. C. Allison and A. Dalgarno, At. Data **1**, 91 (1969).
[14] M. Glass-Maujean, Phys. Rev. A **33**, 342 (1986).
[15] J. A. Beswick and M. Glass-Maujean, Phys. Rev. A **35**, 3339 (1987).
[16] J. E. Mentall and P. M. Guyon, J. Chem. Phys. **67**, 3845 (1977).
[17] M. Glass-Maujean, H. Frohlich, and J. A. Beswick, Phys. Rev. Lett. **61**, 157 (1988).
[18] J. R. Burciaga and A. L. Ford, J. Mol. Spectrosc. **149**, 1 (1991).
[19] P. J. Julienne, Chem. Phys. Lett. **8**, 27 (1971).
[20] H. Gao, C. Jungen, and C. H. Greene, Phys. Rev. A **47**, 4877 (1993).
[21] H. M. J. M. Boesten *et al.*, Phys. Rev. A **55**, 636 (1997).
[22] M. Arndt *et al.*, Phys. Rev. Lett. **79**, 625 (1997).
[23] H. Friedrich, *Theoretical Atomic Physics* (Springer-Verlag, Berlin, 1991), p. 137.
[24] A. Nussenzweig, E. E. Eyler, T. Bergeman, and E. Pollack, Phys. Rev. A **41**, 4944 (1990).
[25] I. Dabrowski and G. Herzberg, Can. J. Phys. **52**, 1110 (1974).
[26] W. C. Stwalley, Chem. Phys. Lett. **6**, 241 (1970).
[27] P. Senn, P. Quadrelli, and K. Dressler, J. Chem. Phys. **89**, 7401 (1988).
[28] L. Wolniewicz and K. Dressler, J. Chem. Phys. **100**, 444 (1994).
[29] W. Kolos and J. Rychlewski, J. Mol. Spectrosc. **62**, 109 (1976).
[30] J. Komasa and A. J. Thakkar, Chem. Phys. Lett. **222**, 65 (1994).